# Development of line-detection algorithms for local positioning in densely seeded crops

V. Fontaine and T.G. Crowe*

*Department of Agricultural and Bioresource Engineering, University of Saskatchewan, Saskatoon, Saskatchewan S7N 5A9, Canada.*
**Email: trever.crowe@usask.ca*

Fontaine, V. and Crowe, T.G. 2006. **Development of line-detection algorithms for local positioning in densely seeded crops**. Canadian Biosystems Engineering/Le génie des biosystèmes au Canada **48**: 7.19 - 7.29**.** Herbicide applications could possibly be reduced if applications were targeted. Targeted applications require prior identification and quantification of the weed population. This task could possibly be done by a weed scout robot. The ability to position a camera over the inter-row space of densely seeded crops will improve the quality of the weed detection. Four line-detection algorithms were evaluated with simulated crop row images. Based on the results, the algorithms were revised and tested again with field images of wheat collected at the 3-leaf, 5-leaf, 2-tiller, and 3-tiller stages. When tested with simulated crop row images, the best algorithm was able to determine the angle of parallel lines in an image with an accuracy of 0.5°, and to find the centreline of an inter-row space within 2.1 mm, even in noisy conditions. When tested with field images containing weeds, the revised version of the same algorithm was able to determine the angle of the inter-row spaces within 11.5° and determined the location of the centreline of an inter-row space with an accuracy of 27.2 mm. Results of all algorithms improved when only the 2-tiller and 3-tiller stages were considered. This paper documents the performance of the line-detection algorithms under lab and field conditions. **Keywords:** line detection, crop row detection, machine vision, autonomous robot, weed scout, weed detection, positioning system.

La quantité d'herbicides appliquée au champ pourrait être diminuée de manière considérable si les applications étaient ciblées. Cela requerrait une identification préalable des mauvaises herbes ainsi qu'une évaluation de leur densité au champ. Cette tâche pourrait être exécutée par un robot autonome. Positionner une caméra au-dessus d'un « entre-rang » en grande culture pourrait simplifier l'estimation automatisée de la densité des populations de mauvaises herbes. Quatre algorithmes capables de reconnaître des patrons linéaires ont été développés. Les algorithmes ont d'abord été évalués avec des images de rangs artificiels élaborées en laboratoire. Après analyse des résultats, les algorithmes ont été modifiés et améliorés pour traiter des images de rangs de blé au champ recueillies aux stades 3-feuilles, 5-feuilles, 2-tiges et 3-tiges. Le meilleur algorithme a déterminé l'angle d'un ensemble de lignes parallèles dans une image avec une précision de 0.5°, et a déterminé l'emplacement de la ligne centrale d'un « entre-rang » avec une précision de 2.1 mm, et ce en présence de bruit simulant des mauvaises herbes. Lorsqu'évaluée à l'aide d'images de rangs de blé en champ incluant des mauvaises herbes, la seconde version du même algorithme a déterminé l'angle des rangs avec une précision de 11.5° et a identifié la ligne centrale d'un entre-rang avec une précision de 27.2 mm. La performance de tous les algorithmes s'est améliorée lorsque les stades 2-tiges et 3-tiges seulement ont été considérés dans l'analyse. Cet article rapporte les résultats détaillés de chaque algorithme. **Mots-clés**: détection de lignes, détection de rangs, vision artificielle, robot autonome, détection des mauvaises herbes, système de positionnement.

## INTRODUCTION

In recent decades, chemical application has become a major environmental issue in agriculture. In addition to their potential adverse effects on the environment, agricultural chemicals can represent a major economic input for producers. Quantities of herbicides used could be reduced if applications were targeted, i.e. if chemicals were applied at specific locations in the field. To implement site-specific applications, weed infestations in the field must be located and quantified. The conventional method involves producers or paid scouts visually inspecting fields. With recent advances in machine vision and control, this time-consuming weed scouting could possibly be done by a robot or autonomous weed scout.

Different autonomous vehicles have been developed for agricultural applications. Researchers at the Danish Institute of Agricultural Sciences (Horsens, Denmark) and Aalborg University (Aalborg, Denmark) have reported on an autonomous weed-mapping vehicle. The vehicle travels from waypoint to waypoint, similar to the approach presented by Palmer and Wild (2000), to generate a weed map. During operation of the Danish system, a row guidance sensor (Bak 2001) modifies the vehicle's trajectory to avoid causing damage to the crop.

Åstrand and Baerveldt (1999a, 1999b, 2001, 2002, 2003) described a row-following autonomous robot for the purpose of mechanical weed control. The robot, designed to work in high weed density conditions, followed a crop row and included a mechanical tool to remove the weeds growing between each plant of the row. The row-following system (Åstrand and Baerveldt 1999a, 1999b, 2001), was based on the Hough Transform, and when it was tested with images of sugar beets and rape, the algorithm's offset error was 60 to 120 mm. In these images, the weed density was more than three weeds per crop plant, and the rows were widely spaced (0.48 m).

Researchers at the Silsoe Research Institute (Silsoe, UK) worked for several years to develop an autonomous crop protection vehicle. This vehicle, mostly tested with cauliflower, followed crop rows and spot sprayed the plants individually. Marchant et al. (1997) described the row-tracking algorithm, based on the Hough Transform, which proved to be very robust and tolerant of missing plants within the rows and presence of outliers.

Functionally, a weed scout robot would be required to identify weeds growing within a crop row and in the space

between the rows (inter-row space). Different challenges are associated with each situation. The identification of weeds within crop rows requires crop row detection and species discrimination, while identifying weeds growing in the inter-row space merely requires crop row recognition.

In any research involving plant discrimination, segmentation of the image is required prior to processing. The goal of segmentation is to provide the line detection system with a partially processed image that includes only plants, an exercise that is complicated by variations in lighting quality and distribution. Images can also contain noise from straw, rocks, and weeds in the inter-row spaces. A number of machine vision researchers, including Marchant et al. (1997) and Reid and Searcy (1986, 1987a, 1987b, 1988, 1991) installed near-infrared filters on cameras to enhance contrast between plants and background, which simplified the segmentation process.

A variety of attempts to define row orientation has been reported. Reid and Searcy (1991) evaluated the Hough Transform, but their efforts were mainly focused on a heuristic line detection algorithm which performed a run-length encoding procedure to find middle points on each row. Billingsley and Schoenfisch (1997) used a technique very similar to regression analysis for line detection, and Slaughter et al. (1997) tested a linear regression and three statistical estimates of central tendency, i.e. the mode, the mean, and the median.

Most of the above-mentioned projects focused on emerging crops in widely-spaced rows. The performance of row-detection systems for the purposes of weed detection in older crops, especially those that are densely seeded crops, is not well documented in the literature. Young crops in narrowly-spaced rows will present challenges in early stages when non-uniform seedling emergence may present discontinuous rows. Discrimination of individual rows will also be more complex as the crop matures and the plants tend to occlude the inter-row spaces.

The weed scout envisioned in the present project would focus mainly on detecting weeds growing in the inter-row space. The weed scout could be required to work under varying lighting conditions or in a partially closed canopy. In such situations, the use of a local positioning system equipped with an illumination chamber or a canopy-opening tool would improve the weed detection accuracy. The weed scout could also be used for spot spraying, mechanical weeding, soil sampling, and detection of insects and diseases. These actions would be facilitated by positioning a tool, end-effector, or camera either over the crop row or over the inter-row space.

## OBJECTIVES

The general objective of this project was to contribute to the development of an autonomous weed scout by developing and testing four line-detection algorithms capable of determining the position and orientation of a camera with respect to crop rows. The specific objectives were:

1. to evaluate the line-detection algorithms with images of artificial rows,
2. to incorporate changes to the line-detection algorithms to allow them to process field images, and
3. to evaluate the algorithms' performance with field images of crop rows, with and without weeds.

The criterion used to evaluate the algorithms was their accuracy in determining:

1. the angle of a line pattern, and
2. the position (x, y) of a point on the centreline of an inter-row space.

## MATERIALS and METHOD

### Evaluation with images of artificial crop rows

Four line detection algorithms were created, each one using a different image processing or pattern recognition technique. The algorithms are referred to as the Linear Regression (LR), the Hough Transform (HT), the Stripe Analysis (SA) and the Blob Analysis (BA) algorithms. The algorithms were coded in Microsoft Visual Basic 6.0 and utilized commands of a commercial imaging library (Matrox Imaging Library version 4.0, Matrox Electronics Ltd., Dorval, QC). The algorithms calculated the angle of the rows within the captured image and the location of a point (x, y) on the centreline of an inter-row space.

The first version of each algorithm was evaluated using images of artificial crop rows, parallel black stripes on a white background with and without weed-simulating noise. Testing the algorithms with perfectly straight lines without noise revealed the algorithms' performance under ideal conditions. Susequent testing with images of plants grown in field conditions revealed some of the challenges involved in processing field images.

The LR and HT algorithms shared two image recognition steps prior to line detection: edge detection and clustering. Edge detection was conducted by searching for pixel value transitions (255 to 0 or 0 to 255) along rows and columns of pixels. The centre points of black stripes were then defined as the points midway between successive 255-0 and 0-255 transitions, or runs. The rows and columns considered in the search were separated by 19 pixels to reduce volume of information and computational requirements. The minimum row width tested was 51 mm, therefore, the edge detection step ignored runs of less than 15 pixels (21 mm), because they were most likely patches of simulated weeds. Figure 1 presents an example of the edge detection along the rows and columns of pixels.

In cases when the stripes in the image were either horizontal or vertical, there would not be any transitions found when the edge detection was performed on the rows and columns of pixels, respectively. To overcome these situations, the number of centre points found after completing each centre point search was recorded. The search that resulted in the greatest number of centre points was used in subsequent analysis.

A clustering technique, termed the Similarity Matrix (Meisel 1972), was used to define the stripes of which the points were members. This method, similar to the Nearest-Neighbour method (Meisel 1972), defined the neighbours of each centre based on the Euclidean distance, which was set to 40 pixels (57 mm). This number was based on the number of rows and columns of pixels considered in the search (1 row or column every 20). Only clusters of more than nine centre points were considered in the subsequent processing steps. Smaller groups may represent simulated weed patches or portions of a row, which could lead to false results (a longitudinal cluster composed of nine centre points spread out at intervals of 40

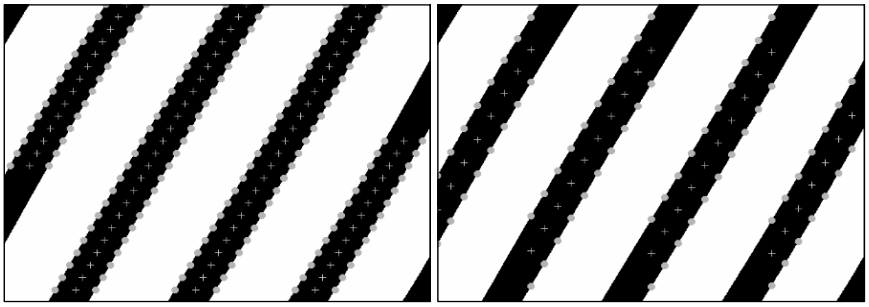

(a) (b)

**Fig. 1. Edge detection along the rows (a) and columns (b) of pixels. ● = stripe edge; + = centre point of black stripe.**

pixels would be 360 pixels long, which is just over half the width of a 640 x 480 pixels image).

The LR algorithm performed a linear regression on each cluster of centre points to determine the equation describing each row. With a conventional linear regression, it was impossible to describe a vertical line because its slope was infinite. In such cases, the dependent and independent variables in the regression were swapped. The algorithm decided which regression (conventional or inverse) should be performed based on what centre point search (along the rows or columns of pixels) provided the highest number of centre points, which was an indication of the angle of the crop rows (see Fig. 1).

The HT algorithm calculated every possible line passing through every centre point of each cluster found. The lines were described using the normal space (ρ, θ), as suggested by Duda and Hart (1972). These equations were put into an accumulator and the most "popular" equation was the one passing through the greatest number of centre points of the cluster. Only clusters where at least three centre points contributed to the "most popular" equation were considered in subsequent analysis. The excluded clusters probably did not present a longitudinal profile and were likely simulated weed patches.

The SA algorithm incorporated commands from an imaging library (Matrox Imaging Library version 4.0, Matrox Electronics Ltd., Dorval, QC) to find a vertical white stripe pattern (i.e. an inter-row space) in the image processed. The stripe width was defined as 90 pixels (129 mm) with a variation of 40 pixels (57 mm) based on the images processed. The search was conducted in a region (search box) of 330 pixels by 330 pixels centred in the image. The search box was then rotated about its centre in increments of 4º, within a range of 0 to 180º. At each angle, the search was performed again and a confidence score was calculated based on the geometric constraints specified in the program, the stripe width for example. The angle presenting the highest confidence score was used for a finer search by step increments of 0.2º. After the stripe feature was located, the algorithm determined the position of its centre. The orientation of the white stripe was given by the angle of the search box presenting the highest confidence score.

The BA algorithm used the intrinsic blob analysis commands of the imaging library. A blob analysis is an image processing operation that finds and characterizes regions of contiguous pixels of the same value in a binarized image. The algorithm searched for white blobs (inter-row spaces) of more than 200 pixels, as smaller blobs could represent noise in the crop rows. Once the blobs were identified, the algorithm determined the angle of their principal axes and the location of their centre of gravity. For a perfectly straight white stripe, the centre of gravity of the blob was over the centreline of the white stripe, and the angle was representative of the angle of the inter-row spaces. The algorithm returned the angle and centre of gravity of the blob closest to the centre of the image.

To simulate crop rows, different line patterns were built. A line pattern was a set of parallel black lines enclosed in a 1.19-m diameter circle on a white background. The black lines represented the crop rows, and the white spaces were the inter-row spaces. To simulate a wide range of situations in the field, each pattern presented different values of row width (RW), 51 or 76 mm, row spacing (RS), 152 or 229 mm, and offset from the center, 0, ¼, ½, or ¾ of the row spacing value. The offset was the perpendicular distance from the centre of the circle to the middle of the nearest white row to the right-hand side. A total of 16 different patterns was prepared.

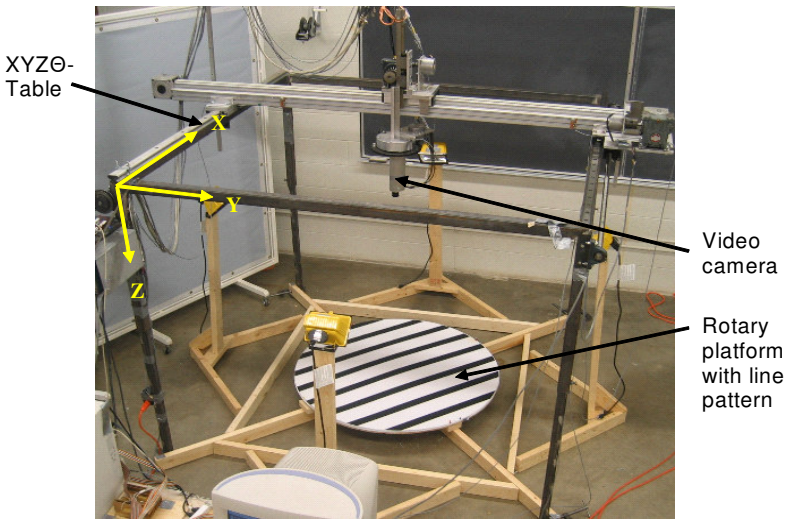


**Fig. 2. Line-detection algorithm testing set.**

An RGB video camera (Model 2200, Cohu Inc., San Diego, CA) and a framegrabber (Meteor RGB, Matrox Electronics Ltd., Dorval, QC) installed in a microcomputer (Pentium III 833 MHz) recorded the artificial crop row images with a resolution of 640 x 480 pixels. The camera was equipped with a lens of 8.5-mm fixed focal length (Computar, Tokyo, Japan). A table capable of positioning an end effector in three axes and rotating about the vertical axis (XYZ-θ table) was used as the camera stand (Fig. 2). The camera was positioned over the centre of the line pattern at a height of 1.22 m, viewing vertically downward. This resulted in an image size of 0.92 x 0.69 m, thus a resolution of 10 mm per 7 pixels.

In the test procedure, a pattern was chosen randomly, fixed on a rotary horizontal platform, and rotated to a randomly assigned angle, one of 0, 30, 90, 120, or 150° clockwise from the vertical orientation in the images. The testing set was calibrated so that the columns of pixels in images were parallel to the lines when the platform was at 0°. Two images were acquired, one with only the rows in the field of view and a second with simulated weeds. The simulated weeds consisted of scattered sunflower seeds and pieces of black foam cut in different shapes of approximately 1700 $mm^2$ on average. The overall surface area occupied by the "weeds" was approximately 0.05 $m^2$ in each image. A total of 288 images was gathered under "weed free" conditions (2 RW x 2 RS x 4 offsets x 6 angles x 3 replicates) and 288 under "weedy" conditions. The complete database of images included 576 images.

Each image was processed by the four line-detection algorithms. The performance of the algorithms was quantified in terms of error in the angle of rows found and positional error. The error in row angle was calculated as the absolute value of the difference between the angle found by the algorithm and the angle of the line pattern. The positional error was defined as the perpendicular distance from the point (found by the algorithm) describing the inter-row space centreline to the closest centreline of a white stripe. If the distance was 0, the target position according to the algorithm was exactly over the centreline of a white stripe.

**Modifications to the line-detection algorithms**

In the field, crop rows will seldom be straight with parallel sharp edges. Moreover, plants may not be easily segmented from the background, resulting in discontinuous rows in the images. It is thus reasonable to expect that the first versions of the algorithms, which were designed to process images of parallel stripes, will perform differently when processing field images. To allow processing field images with acceptable results, the algorithms were modified.

A pre-processor stage was added prior to the line-detection algorithms to produce images similar to the artificial crop row images, i.e. continuous rows with distinct edges and a minimum amount of noise in the inter-row spaces. The pre-processing step consisted of a series of automated blob fillings, dilations, and erosions of the plant material in the image, preceded by a filtering operation to remove noise. To be able to pre-process a wide range of field images, the pre-processing step had to be adaptable to the growth stage of the plants. Younger plants required more dilations and gap fillings to create a continuous stripe, whereas older plants covering an important part of the inter-row spaces required more erosions. The operations of the pre-processor were set by the percentage of plant material in the image (ratio of the number of black pixels in the image to the total number of pixels) not on the growth stage. Five pre-processing algorithms were designed to suit images containing less than 12%, 12 to less than 20%, 20 to less than 32%, 32 to less than 50%, and 50% and more of plant material.

The width of inter-row spaces in field images was unknown, unlike in the images of artificial rows. Thus, the SA algorithm was revised so that the width of the white stripe to find was defined as 100 pixels with a variation of 80 pixels, allowing a wider range of images to be successfully processed. The search box was also reduced to 290 pixels by 290 pixels to fit the field images used for testing, which were 414 pixels by 414 pixels.

The revised BA algorithm searched for white blobs (inter-row spaces) of more than 2500 pixels, as opposed to 200 pixels in the first version. It was believed that blobs of more than 2500 pixels had a higher probability of representing the inter-row space, thus leading to better results. Also, the second version calculated the product of the area of each blob by its elongation. The blob featuring the highest product was retained for further analysis, because it was well correlated with the shape of an inter-row space.

In the second version of the LR and HT algorithms, the edge detection step found centre points in the inter-row spaces instead of the rows. In processing, the field images, being smaller than the artificial crop row images, the edge detection was performed on rows and columns of pixels separated by 14 pixels instead of 19. The Euclidean distance in the Similarity Matrix was also reduced to 30 pixels to adapt to the new distance between the rows and columns of pixels considered in the edge detection.

The HT algorithm was applied to clusters of more than seven centre points. Clusters of seven and fewer centre points were considered poor representatives of the inter-row spaces (the maximum length of a cluster with seven centres separated by 30 pixels was 210 pixels, half of the width of the 414 x 414 pixels image). The LR algorithm excluded the same category of clusters and also excluded clusters of more than 35 centres because they had a high probability of spanning over two inter-row spaces through a discontinuous row. In the case of the LR algorithm, the cluster selected as most representative of the inter-row space had the highest product of the $R^2$ value of the regression by the number of centre points included in that cluster. In the case of the HT algorithm, the cluster with the maximum number of centre points contributing to its "most popular" equation was selected.

**Evaluation with field images**

The revised algorithms were tested with binarized field images that were acquired at random locations in a field of wheat, at 3-leaf, 5-leaf, 2-tiller, and 3-tiller stages. Figure 3 presents an example of each stage. The images were acquired over a period of 24 days, generally between 10:00 and 17:30h. Images were acquired using two monochrome cameras installed adjacently. One camera, subsequently referred to as the NIR camera, (XC-EI50, Sony Corporation, Tokyo, Japan) had increased sensitivity in the near infrared up to 1000 nm. The second camera (XC-ES50, Sony Corporation, Tokyo, Japan) was sensitive to the visible light spectrum (400 to 750 nm) and was referred to as the RED camera.

The cameras were equipped with identical 6-mm fixed focal length lenses. Each camera lens was fitted with a filter to isolate a particular wavelength band. The RED camera was fitted with a narrow bandpass interference filter to capture red reflectance centered about 640 nm with a full width at half maximum bandwidth (FWHM) of 11.4 nm. The NIR camera was fitted with a long-pass filter with a cut-off wavelength of 830 nm. The infrared long-pass filter combined with the decreased sensitivity of the CCD sensor above 900 nm created an effective broad bandpass response centered about 860 nm for the NIR camera. At each location, only the intersecting area of 414 pixels by 414 pixels of the two original images was considered in subsequent

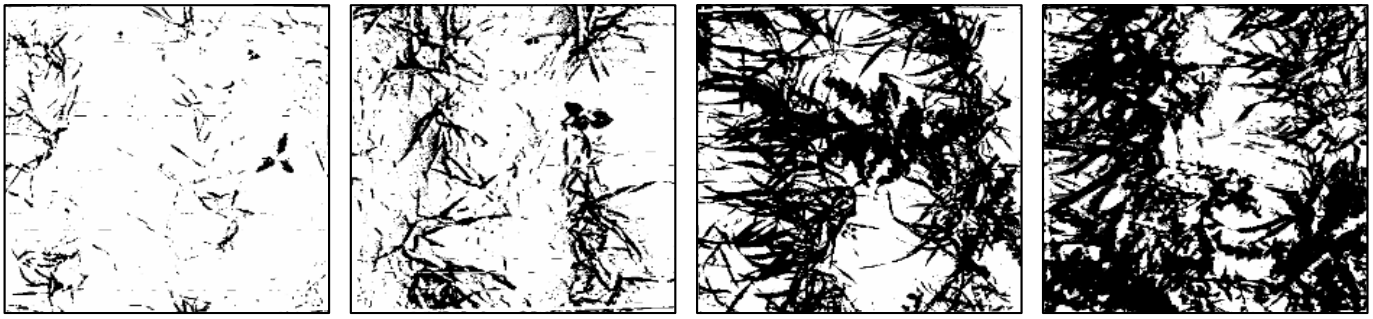

(a) (b) (c) (d)

**Fig. 3. Binarized field images at different stages of growth: (a) 3-leaf; (b) 5-leaf; (c) 2-tiller; and (d) 3-tiller.**

**Table 1. Mean plant material percentage (%) in field images for each growth stage.**

| Stage of growth | Weeded images | Weedy images | Difference |
|---|---|---|---|
| 3-leaf | 3.4 | 7.2 | 3.7 |
| 5-leaf | 13.4 | 20.7 | 7.3 |
| 2-tiller | 26.6 | 34.8 | 8.1 |
| 3-tiller | 39.9 | 52.8 | 12.9 |
| Mean | | | 8.0 |

analysis. For each pixel in the intersecting image, the NIR/Red ratio was calculated and a threshold was used to obtain binarized images. Based on the work by Baron (2005), it was hypothesised that the NIR/Red ratio was an efficient method to extract living plants from background (soil, rocks, dead plant material). This procedure also eliminated shadows caused by the angle of the sun.

At every location, an image containing naturally occurring weeds in the rows and inter-row spaces was acquired. Then the weeds were manually removed from the area and another image was acquired. Fifteen "weedy" and 15 "weeded" images were collected at each stage of growth, for a total of 120 images. Table 1 describes the data set of field images in terms of percentage of plant material for each stage of growth. On average, the weeds represented 8% of the weedy images. This value was calculated as the difference between the percentage of black pixels (plant material) in the "weedy" and "weeded" image at each location. Table 2 classifies every field image according to its percentage of plant material. The evaluation of the plant material in the images was influenced by the manual weeding of the area, which sometimes caused more crop material to be visible in the "weeded" image. This situation may have resulted in an equal or greater number of black pixels found in the "weeded" image in comparison to the corresponding "weedy" image, even though the weeds were removed. The wind may have also moved the leaves and revealed more "good" plant material in the "weeded" image acquired.

Crop rows in the images were often discontinuous and weeds were sometimes contiguous with two crop rows. A visual inspection of the field images revealed that either of these two situations occurred in 26 images out of 30 in the 3-leaf stage, 20 in the 5-leaf stage, 8 in the 2-tiller stage and 7 in the 3-tiller stage. Field images contained two or three crop rows, so that at least one entire inter-row space was visible and limited by two visible crop rows. The rows were oriented approximately parallel to the sides of the image. The row spacing was 300 mm and the resolution of the image was 1 pixel = 1.5 mm at a reference plane 30 mm above the ground.

**Table 2. Classification of field images according to their plant density.**

| Stage of growth | | Plant material in image (%) | | | | | Total |
|---|---|---|---|---|---|---|---|
| | | [0, 12[ | [12, 20[ | [20, 32[ | [32, 50[ | [50, 100] | |
| 3-leaf | Weeded | 15 | - | - | - | - | 15 |
| | Weedy | 12 | 3 | - | - | - | 15 |
| 5-leaf | Weeded | 3 | 12 | - | - | - | 15 |
| | Weedy | 1 | 8 | 5 | 1 | - | 15 |
| 2-tiller | Weeded | - | 3 | 9 | 3 | - | 15 |
| | Weedy | - | 1 | 6 | 7 | 1 | 15 |
| 3-tiller | Weeded | - | - | 3 | 11 | 1 | 15 |
| | Weedy | - | - | 1 | 4 | 10 | 15 |
| | Total | 31 | 27 | 24 | 26 | 12 | 120 |

The binarized field images were processed by the second version of each algorithm. The algorithms determined the angle of an inter-row space and a point (x, y) on the centreline of that inter-row space. The "actual" angle and centreline location of each inter-row space in each image was estimated manually. The error in row angle was defined as the absolute value of the difference between the angle found by the algorithm and the "actual" angle of the inter-row space. The positional error was defined as the perpendicular distance from the point (found by the algorithm) describing the inter-row space centreline to the closest inter-row space centreline.

**Table 3. Error on the determination of the row angle (°) in simulated crop rows (n = 288).**

| Algorithm | Noise-free image LSmean ± SD | Noisy images LSmean ± SD | Increase in LSmean‡(%) |
|---|---|---|---|
| Blob Analysis v1.0 | 0.47 a ± 0.36 | 0.96 a ± 4.28 | 104 |
| Hough Transform v1.0 | 0.49 ab ± 0.43 | 0.85 a ± 6.08 | 73 |
| Stripe Analysis v1.0 | 0.54 bc ± 0.36 | 0.54 a ± 0.41 | 0 |
| Linear Regression v1.0 | 0.56 c ± 0.36 | 1.08 b ± 1.13 | 93 |

* Means grouped according to type of image (noise-free or noisy)
† Grouping is based on an unpaired t-test on the equality of means (α = 0.05)
‡ Increase in LSmean = [(LSmean noisy - LSmean noise-free)/LSmean noise-free]*100

## DATA ANALYSIS and DISCUSSION

### Determination of stripe orientation

**Artificial crop row images** Mean errors for stripe angle determination were calculated for each algorithm when analyzing images of simulated crop rows (Table 3). Differences in means when processing noisy images were not significant, however the BA algorithm posted the least error of 0.47° when analyzing noise-free images. The worst algorithm, using LR, had an error mean of 0.56º. The variation in the data was consistent over the four algorithms, with a standard deviation of approximately 0.4º. Mean errors were larger when the noisy images were analysed. The greatest increase in mean error (relative to the mean errors using the noise-free images) was posted using the BA algorithm, with a 104% increase (0.96°). Standard deviations also generally increased with the addition of noise, especially for the BA and the HT algorithms. The worst algorithm was again the LR algorithm, with a mean error of 1.08°. It is interesting to note that the Stripe algorithm mean wasn't affected at all by the noise in the images. The mean error of this algorithm (0.54º) remained unchanged, while the standard deviation increased slightly.

The results of analyses using noise-free versus noisy images were consistent with expectations. The commands from the imaging library used to create the SA algorithm were known from experience to be robust. It was not surprising to see this algorithm performing the same way with or without noise because this noise was randomly scattered in the image and did not nearly resemble the straight edges for which the algorithm was searching. Investigation of the data of the BA algorithm revealed that the error in the angle found in three images was more than 20°. Without these data, the mean error and standard deviation decreased to 0.57° ± 0.44. Therefore, we can conclude that when processing noisy images of artificial crop rows, this algorithm was generally as accurate as the SA algorithm, but the BA algorithm was predictably more sensitive to noise. The angle of the inter-row spaces, or blobs, was computed from the relative positions of the white pixels forming the blob. If the noise was asymmetrical in the blob, the orientation of the blob's longest axis may have been misleading. In the specific case of the images with an error greater than 20°, simulated weed patches created "bridges" between two rows (Fig. 4) resulting in small white blobs within an inter-row space. Similar situations will probably cause important errors in field images. Published literature (Marchant et al. 1997) suggested that the Hough Transform is tolerant to a small amount of outliers in the linear pattern (noise). With a 73% increase in mean error when noise was added to the images, it could be concluded that the data from this work were not consistent with the literature. However, further investigation of the data revealed that one image had a great influence on the results. In that image, presented in Fig. 5, the error (103.4°) can be explained by the particular positions of the weeds, which caused the Similarity Matrix to form three groups instead of one. A second analysis performed without this image in the data revealed that the mean error and standard deviation decreased to 0.49° ± 0.42. The results of the HT algorithm, then exactly

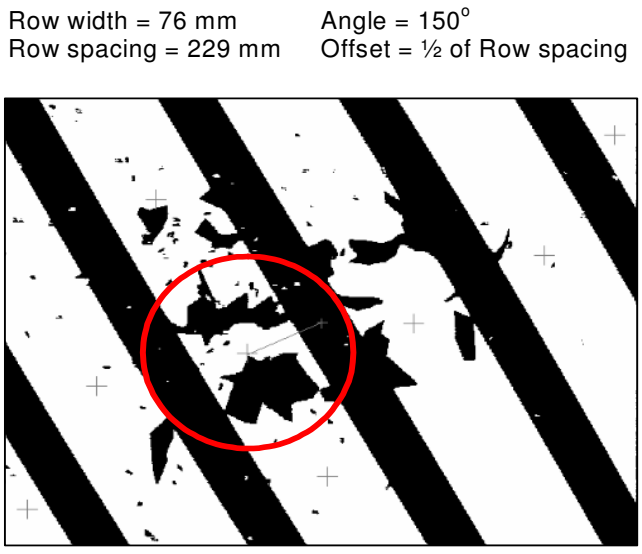


**Fig. 4. Noise creating a white blob within inter-row space.**

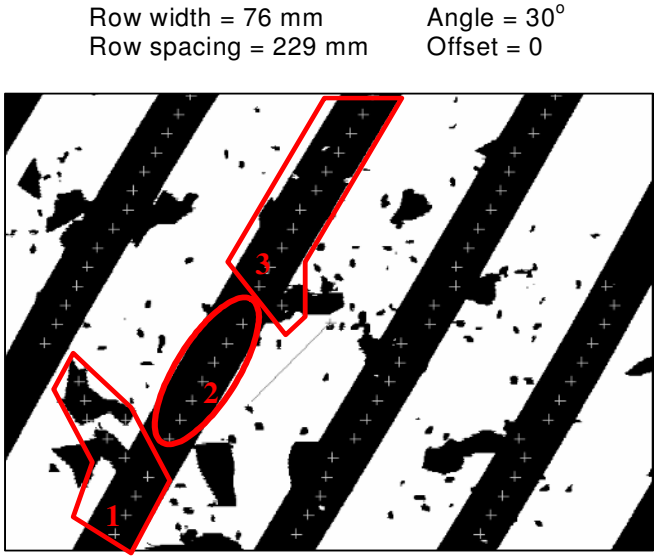


**Fig. 5. Three clusters formed in the same row.**

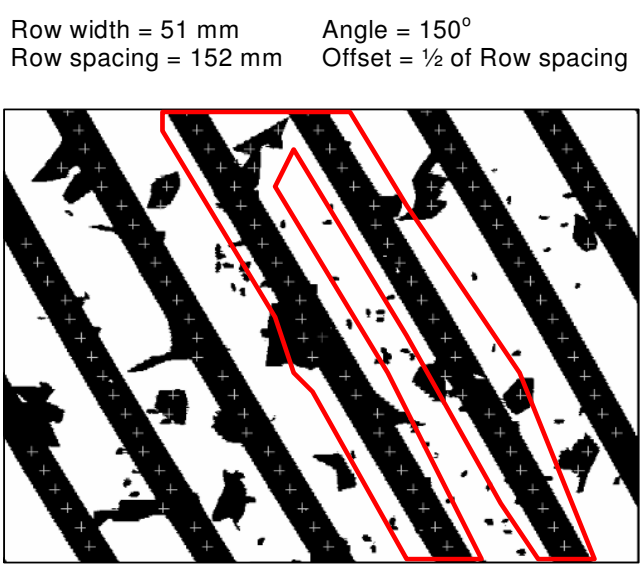


**Fig. 6. Two rows clustered as one.**

the same with and without noise, were consistent with the literature. "Bridges" between two adjacent rows also proved problematic for the LR algorithm when two rows were clustered as one (Fig. 6).

**Field images** The LR and HT algorithms required that field images met a certain number of criteria to compute a result. For example, only clusters including more than seven centre points were considered. Certain field images didn't meet these requirements and were discarded by the algorithms. Results are presented in Table 4. The SA algorithm performed best and it determined the angle of crop rows with an accuracy of 8° in weeded images and 11.5° in weedy images. The second best algorithm was the BA algorithm, but its error rate in weeded images was twice that of the SA algorithm. The BA algorithm was the most consistent among weeded and weedy images. This algorithm presented a mean increase of 9% when processing weedy images. The consistency of the HT and LR algorithms also improved compared to their implementation with the artificial crop rows. Variation in the data was notable with standard deviations of more than 20°.

Results from images of artificial crop rows suggested that discontinuity in inter-row spaces or weeds creating "bridges"

**Fig. 7. Example of error in determination of stripe location by the Stripe Analysis algorithm in a field image: + = stripe centre; ● = stripe edges.**

between crop rows could lead to false results in field images. Results from the SA algorithm showed that this challenge remained. Four weeded images and six weedy images presented an error in angle greater than 75°. When these images were removed from the data set, the LS means and standard deviations decreased to 2.2° ± 2.2 for weeded images and 3.2° ± 8.0 for weedy images. The errors in those images were caused by the roughness of the crop edges and discontinuity in the rows. In these cases, the stripe having the highest confidence score was found within a crop row, as in Fig. 7. The BA algorithm was particularly sensitive to discontinuities. Missing plants in crop rows caused the white pixels of two inter-row spaces to be contiguous. They were then classified as one blob, and the angle of the blob wasn't representative of the angle of the inter-row spaces. Among the images processed by the LR and HT algorithms, two problematic situations were identified. First and foremost, although the pre-processing step partially smoothened the original crop edges, the resulting edges were still considerably rough. In some images, this resulted in a slightly greater number of inter-row space centres to be found along the columns of pixels than the rows in the edge detection step. Therefore, the similarity matrix formed clusters from the set of centre points found along the columns of pixels. The clusters formed did not represent the inter-row spaces. Figure 8 presents an image where the centre points were found in the edge detection along the rows (a) and columns (b) of

**Table 4. Error in the determination of the row angle (°) in field images.**

| Algorithm | Weeded area | | Weedy area | | Increase in LSmean‡(%) |
|---|---|---|---|---|---|
| | n | LSmean ± SD | n | LSmean ± SD | |
| Stripe Analysis v2.0 | 60 | 8.04 a ± 22.00 | 60 | 11.49 a ± 26.24 | 43 |
| Blob Analysis v2.0 | 60 | 16.57 b ± 20.85 | 60 | 17.98 ab ± 21.54 | 9 |
| Linear Regression v2.0 | 53 | 20.79 b ± 26.99 | 55 | 24.95 b ± 27.39 | 20 |
| Hough Transform v2.0 | 53 | 21.03 b ± 26.66 | 54 | 24.41 b ± 27.99 | 16 |

* Means grouped according to type of image (weeded or weedy)
† Grouping is based on an unpaired t-test on the equality of means ($\alpha = 0.05$)
‡ Increase in LSmean = [(LSmean weedy - LSmean weeded)/LSmean weeded]*100

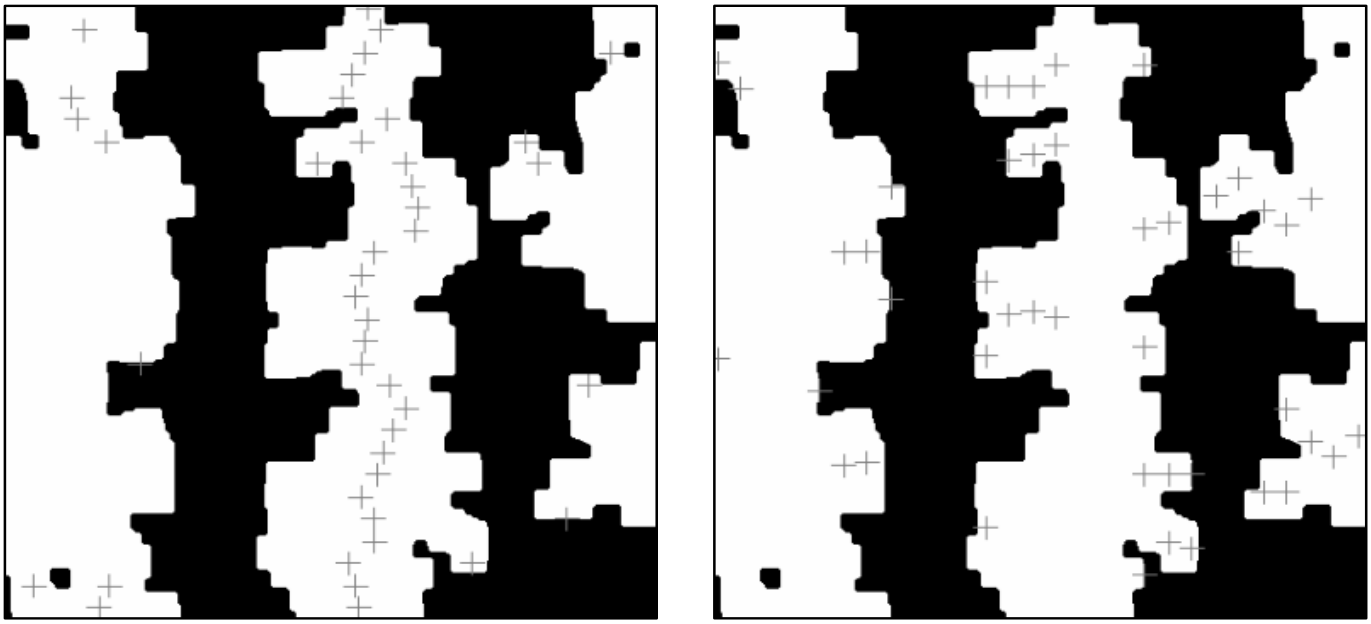

(a) (b)

**Fig. 8. Image representing the centre points (+) found in edge detection along the rows (a) and columns (b) of pixels in field images.**

pixels. The second problematic situation, which was often a consequence of the first, arose when no cluster included more than seven centres. When this was the case, the LR and HT algorithms were not performed on the results of the Similarity Matrix. Therefore, no results were available for these images. Clusters where only two centre points contributed to the "most popular" equation in the Hough Transform did not provide a result either. In each case, the selection of the edge detection along the rows of pixels would have probably solved the problem.

For applications in a weed scout robot, an orientation error of less than 15° was arbitrarily deemed acceptable. An error greater than 15° would probably cause damage to the plants when positioning a sampling tool or other equipment relative to the row orientation. From this perspective, only the SA algorithm would be suitable for use in field conditions.

### Determination of stripe location

**Artificial crop row images** Mean errors were also calculated in determining the location of inter-row spaces in noise-free and noisy images (Table 5). Under noise-free conditions, the HT and LR algorithms performed equally well with mean errors near 1.3 mm. The average error for the other algorithms was less than 2.6 mm. While the SA and BA algorithms provided good results with the addition of noise, the LR and HT algorithms were dramatically affected. The mean errors of these algorithms increased by more than 400 and 500%, respectively. Based on the standard deviations, variation in the data was a problem for the LR and the HT algorithms. These algorithms presented a variation of 265 and 194% of the mean, respectively. The fact that both algorithms were affected by the addition of noise might be due to the clustering step. Investigation of the data revealed that the problematic situations found in determining stripe orientation (more than one cluster per row and two rows in the same cluster) also caused notable errors in the determination of the stripe location.

Again, it was observed that the SA algorithm mean error (2.1 mm) and standard deviation weren't affected by the addition of noise, which made it applicable to use in field conditions. Results of the Blob algorithm were also acceptable (2.6 mm in noise-free conditions and 3.3 mm in noisy conditions). However, small blobs created by the "weeds" were again the reason for poor positioning results.

**Table 5. Error in the determination of the inter-row space location (mm) in simulated crop rows (n = 288).**

| Algorithm | Noise-free image LSmean ± SD | Noisy images LSmean ± SD | Increase in LSmean‡(%) |
|---|---|---|---|
| Hough Transform v1.0 | 1.3 a ± 1.3 | 6.5 a ± 17.2 | 411 |
| Linear Regression v1.0 | 1.4 a ± 1.2 | 8.5 a ± 16.4 | 509 |
| Stripe Analysis v1.0 | 2.1 b ± 1.2 | 2.1 b ± 1.3 | 2 |
| Blob Analysis v1.0 | 2.6 c ± 1.7 | 3.3 c ± 5.3 | 24 |

* Means grouped according to type of image (noise-free or noisy)
† Grouping is based on an unpaired t-test on the equality of means (α = 0.05)
‡ Increase in LSmean = [(LSmean noisy - LSmean noise-free)/LSmean noise-free]*100

**Field images** Results with field images were consistent with expectations. The SA algorithm was again the most accurate in weeded and weedy images, with positioning errors of 22.6 mm and 27.2 mm (Table 6). The performance of the LR versus the HT algorithm was similar, with a slightly better performance of the LR algorithm in weeded images (28.9 mm).

The BA algorithm performed better in weedy images, which was not consistent

**Table 6. Error in the determination of the inter-row space location (mm) in field images.**

| Algorithm | Weeded area | | Weedy area | | Increase in LSmean‡(%) |
|---|---|---|---|---|---|
| | n | LSmean ± SD | n | LSmean ± SD | |
| Stripe Analysis v2.0 | 60 | 22.6 a ± 30.1 | 60 | 27.2 a ± 31.6 | 20 |
| Linear Regression v2.0 | 53 | 28.9 a ± 32.9 | 55 | 45.0 b ± 47.3 | 56 |
| Hough Transform v2.0 | 53 | 33.5 a ± 31.3 | 54 | 45.6 b ± 37.0 | 36 |
| Blob Analysis v2.0 | 60 | 72.3 b ± 58.5 | 60 | 58.7 b ± 48.7 | -19 |

* Means grouped according to type of image (weeded or weedy)
† Grouping is based on an unpaired t-test on the equality of means ($\alpha = 0.05$)
‡ Increase in LSmean = [(LSmean weedy - LSmean weeded)/LSmean weeded]*100

**Table 7. Error in the determination of the inter-row space location (mm) in field images, 2-tiller and 3-tiller growth stages only.**

| Algorithm | Weeded image | | Weedy images | | Increase in LSmean‡(%) |
|---|---|---|---|---|---|
| | n | LSmean ± SD | n | LSmean ± SD | |
| Stripe Analysis v2.0 | 30 | 11.0 a ± 16.6 | 30 | 12.5 a ± 16.4 | 13 |
| Blob Analysis v2.0 | 30 | 24.6 b ± 29.7 | 30 | 28.4 b ± 27.1 | 15 |
| Linear Regression v2.0 | 25 | 15.5 ab ± 14.4 | 27 | 23.2 b ± 21.4 | 50 |
| Hough Transform v2.0 | 25 | 21.6 b ± 15.9 | 27 | 23.7 b ± 19.7 | 10 |

* Means grouped according to type of image (weeded or weedy)
† Grouping is based on an unpaired t-test on the equality of means ($\alpha = 0.05$)
‡ Increase in LSmean = [(LSmean weedy - LSmean weeded)/LSmean weeded]*100

with previous results. This was again a result of the weakness of the algorithm: images where crop rows were discontinuous. The removal of certain weed plants created gaps in the rows. Two inter-row spaces were included in the same blob, which was then selected as the best representative of an inter-row space because of its area. Moreover, in certain cases, removing weeds significantly decreased the estimated amount of plant material in the image. The weedy and weeded images may then have been pre-processed differently. The main cause of errors in the SA results was the rough crop row edges. Plant material (leaves and weeds) outside of the rows' linear pattern also caused positioning errors because it provided an edge to be used by the SA algorithm. The analysis using artificial crop row images suggested that discontinuity in the rows and inter-row spaces' linear pattern could cause major problems with the LR and the HT algorithms. However, the main problem in determining locations of the inter-row spaces in field images was the rough edges of the rows. The edge detection resulted in a greater number of centres found along the rows of pixels and these centres were then used in subsequent analysis, even though they didn't represent the inter-row spaces.

In the present project, a positional error of more than 10% of the row spacing was not acceptable for two reasons. First, the risk of damage to the plants when positioning a tool would be too high. Second, in narrow-spaced crops (0.15 m), an offset greater than 15 mm would possibly result in the camera being positioned directly over a shady region of the inter-row space, or viewing directly down onto crop leaves. In the present project, field images presented a row spacing of 300 mm. Only the SA algorithm was able to determine the location of an inter-row space centreline in weedy situations with less than 30 mm of error (Table 6).

**Additional analysis in field images**

The field images used in this project covered a wide range of growth stages. Images of the first and last stages of growth were very different in appearance. Therefore, it is reasonable to suggest that they might be analysed differently, and that the algorithms would perform better at specific stages of growth. Positional errors at each stage of growth were calculated for each algorithm. It was observed that two stages of growth always provided the best results: the 2-tiller and 3-tiller stages. This difference in results was probably due to the relatively low proportion of discontinuous crop rows and inter-row spaces in these two stages. Means of positional errors were calculated again considering only these two stages. Table 7 presents the results. When compared to Table 6, which considered all four stages of growth, it is observed that error means decreased significantly. When considering only the 2-tiller and 3-tiller stages, all algorithms were able to determine the location of an inter-row space within the maximum acceptable error of 30 mm. The SA algorithm retained the best results with a positional error in weedy images of 12.5 mm. Mean errors in the angle of the inter-row spaces was generally decreased when only the 2-tiller and 3-tiller stages were considered. The SA and BA algorithms presented an error of approximately 5 and 12° in weedy conditions, respectively (Table 8).

## SUMMARY and RECOMMENDATIONS

The results with images of artificial crop rows indicated how the algorithms would perform with images of perfectly straight line patterns and suggested how they may perform under weedy circumstances. They also revealed certain problems the algorithms would have to face in field images, e.g. variation in the field data. The problematic situations were addressed in the second version of the algorithms.

The most important modification to the algorithms was the addition of a pre-processing step. The objective of this pre-processing step was to produce images that resembled the artificial crop row images. However, the objective was only partially fulfilled. The pre-processing step was unable to adequately smooth the row edges and did not eliminate discontinuity in crop rows and inter-row spaces caused by missing plants and "bridges" of weeds between adjacent rows. These two problems caused the majority of errors for all

**Table 8. Error in the determination of the row angle (°) in field images, 2-tiller and 3-tiller growth stages only.**

| Algorithm | Weeded image | | Weedy images | | Increase in LSmean‡(%) |
|---|---|---|---|---|---|
| | n | LSmean ± SD | n | LSmean ± SD | |
| Stripe Analysis v2.0 | 30 | 5.30 a ± 16.01 | 30 | 12.28 a ± 26.46 | 132 |
| Blob Analysis v2.0 | 30 | 12.37 ab ± 18.22 | 30 | 11.04 a ± 14.85 | -11 |
| Linear Regression v2.0 | 25 | 17.93 b ± 26.94 | 27 | 21.31 a ± 24.99 | 19 |
| Hough Transform v2.0 | 25 | 20.31 b ± 23.35 | 27 | 21.33 a ± 23.54 | 5 |

* Means grouped according to type of image (weeded or weedy)
† Grouping is based on an unpaired t-test on the equality of means ($\alpha = 0.05$)
‡ Increase in LSmean = [(LSmean weedy - LSmean weeded)/LSmean weeded]*100

algorithms. Despite these flaws, it is fair to state that pre-processing the images improved the results of each algorithm in field images. Without that pre-processing step, there would not have been any smooth edges for the SA algorithm to find. The asymmetry of the inter-row spaces and the important number of white blobs found in field images would have confused the BA algorithm. Finally, the edge detection would not have been successful in finding crop rows or inter-row space centres in the LR and HT algorithms. The performance of these two algorithms greatly depended on the clustering method's ability to find the rows.

The difference in results between the laboratory and field evaluation was caused by two factors. First, the field images contained less information than laboratory images, with only two to three rows per image. Second, a large proportion of the field images processed contained discontinuous crop rows or "bridged" inter-row spaces. Capturing a larger area in field images might improve the results. By doing so, a greater number of inter-row spaces would be analysed and a greater portion of the rows would be visible, much like in the laboratory images. The impact of random missing plants and weedy "bridges" on the determination of the location and orientation of inter-row spaces would then be possibly minimized. Another solution would be to perform image processing that would join together discontinuous segments of a row or inter-row space, therefore eliminating discontinuity. Results would also improve if the additional image treatment resulted in distinct crop rows similar to the artificial crop rows analysed in this project.

The heuristic algorithms presented herein can be modified and adapted to different field conditions, e.g. row spacing, which will be known from seeding. The algorithms can be used at different growth stages and do not require prior knowledge of the row width.

## CONCLUSION

The ability of four algorithms to determine the orientation of a set of parallel stripes simulating crop rows in an image and the location of an inter-row space centreline was evaluated in a laboratory setting, with and without weed-simulating noise. All algorithms behaved approximately the same when determining the row orientations in the noise-free images, with an average error of 0.5°. In the same situation, all algorithms could find the centreline of an inter-row space within 2.6 mm. Because of its insensitivity to noise, the SA algorithm was considered the best overall, followed by the BA algorithm. Variation in the data was important.

A second, more robust version of the algorithms was developed based on their evaluation in laboratory conditions. The second versions of the algorithms were tested with binarized images of wheat at four stages of growth, with and without weeds. In weedy images, weeds represented 4 to 13% of the image area. Before detecting the crop rows, each image underwent a sequence of processing steps aimed at removing most of the noise and producing images that resembled as much as possible the laboratory images previously processed. The best algorithm was again the SA algorithm with an orientation error of 11.5° and a positional error of 27.2 mm in weedy conditions over all four stages of growth. All algorithms performed best in the 2-tiller and 3-tiller stages of growth. When considering only these stages, all algorithms presented a positioning error less than 30 mm, which was considered acceptable for use in field conditions. In the same situation, the SA algorithm and the BA algorithm could determine the orientation of crop rows within 12° of error. The main causes of error were discontinuity in the linear pattern of the rows and inter-row spaces and roughness of the row edges. Performances of the LR and the HT algorithms were highly dependent on the clustering and edge detection step. Variation in field images was important.

Future work involves improving the sequence of image processing steps to produce distinct edges and continuous crop rows. Such images are anticipated to produce results similar to those achieved when analyzing artificial crop row images.

## REFERENCES


Åstrand, B. and A.J. Baerveldt. 1999a. Mechatronics in agriculture – Robust recognition of plant rows. In *The 2nd International Conference on Recent Advances in Mechatronics ICRAM'99*, 135-141. Istanbul, Turkey: Boôaziçi University.

Åstrand, B. and A. J. Baerveldt. 1999b. Robust tracking of plant rows using machine vision. In *The Sixth International Conference on Mechatronics and Machine Vision in Practice*, 95-101. Ankara, Turkey: Middle East Technical University.

Åstrand, B. and A.J. Baerveldt. 2001. Design of an agricultural mobile robot for mechanical weed control. In *Proceedings of the Fourth European Workshop on Advanced Mobile Robots Eurobot'01*, 139-146. Lund, Sweden: Lund University.

Åstrand, B. and A.J. Baerveldt. 2002. An agricultural mobile robot with vision-based perception for mechanical weed control. *Autonomous Robots* 13(1):21-35.

Åstrand, B. and A.J. Baerveldt. 2003. A mobile robot for mechanical weed control. *International Sugar Journal* 105:89-95.

Bak, T. 2001. Vision-GPS fusion for guidance of an autonomous vehicle in row crops. In *ION GPS 2001*, 423-451. Fairfax, VA: Institute of Navigation.

Baron, R.J. 2005. Spatial weed distribution determined by ground cover measurements. Unpublished M.Sc. thesis. Saskatoon, SK: University of Saskatchewan, Department of Agricultural and Bioresource Engineering.

Billingsley, J. and M. Schoenfisch. 1997. The successful development of a vision guidance system for agriculture. *Computers and Electronics in Agriculture* 16:147-163.

Duda, R.O. and P.E. Hart. 1972. A generalized Hough Transformation for detecting lines in pictures. *Communications of the ACM* 15:1-15.

Marchant, J.A., T. Hague and N.D. Tillett. 1997. Row-following accuracy of an autonomous vision-guided agricultural vehicle. *Computers and Electronics in Agriculture* 16:165-175.

Meisel, W.S. 1972. *Computer-Oriented Approaches to Pattern Recognition*. New York, NY: Academic Press Inc.

Palmer, R. and D. Wild. 2000. Motorized weed scouting robot: Feasibility and design. Indian Head, SK: Indian Head Agricultural Research Foundation.

Reid, J.F. and S.W. Searcy. 1986. Detecting crop rows using the Hough Transform. ASAE Paper No. 86-3042. St. Joseph, MI: ASABE.

Reid, J.F. and S.W. Searcy. 1987a. Vision-based guidance of an agricultural tractor. *IEEE Control Systems Magazine* 7(2):39-43.

Reid, J.F. and S.W. Searcy. 1987b. Automatic tractor guidance with computer vision. *SAE Technical Paper Series No. 871639*. Warrendale, PA: SAE.

Reid, J.F. and S.W. Searcy. 1988. Algorithm for separating guidance information from row crop images. *Transactions of the ASAE* 31(6):1624-1632.

Reid, J.F. and S.W. Searcy. 1991. An algorithm for computer vision sensing of a row crop guidance directrix. *SAE 1991 Transactions* 100(2):93-105.

Slaughter, D.C., P. Chen and R.G. Curley. 1997. Computer vision guidance system for precision cultivation. ASAE Paper No. 97-1079. St. Joseph, MI: ASABE.